Detailed sensitivity analysis assessment for the determination of the best clay volume model in the shallow offshore area in Suriname.

Raidel F. Djodi[1, *], *Elias R.* Acosta[2], and *James S.* Deering[3]

[1]Staatsolie Maatschappij Suriname N.V, Offshore Directorate, Subsurface Appraisal & Evaluation Team, Paramaribo, Suriname
[2]Staatsolie Maatschappij Suriname N.V, Onshore Directorate, FSS - Formation Evaluation Department, Saramacca, Suriname
[3]Deering Petrophysical Ltd, Chard, United Kingdom

Abstract. Clay minerals in hydrocarbon-bearing reservoirs can impede porous connections and affect various properties such as porosity, water saturation, and permeability. They can also create heterogeneity both vertically and horizontally, making it crucial to determine clay content and principal minerals. A study was conducted in the shallow offshore area of the Guiana-Suriname basin to analyse the clay volume (Vcl) in wells using different clay estimation models. Before this study, different approaches were used to evaluate clay content in the shallow offshore wells, resulting in inconsistent outcomes and significant uncertainties in Vcl across the study area. The objective of this research was to establish a more reliable petrophysical workflow for Vcl calculations. To achieve this objective, a sensitivity analysis was performed using an Excel-based tool called the Vcl Equation Assessment Tool (VCLEAT). Three wells with X-Ray Diffraction (XRD) core analysis were used to find the best match model for the study area, which was then used to calculate Vcl for 26 other wells. The calculated Vcl from various clay models was compared to the Vcl obtained from XRD analysis of 64 Rotary Side Wall Core (RSWC) samples. Input parameters' statistics were determined from histograms constructed for each XRD sample depth, clean sand interval, and shaly interval in the geological interval of interest. These statistics were used to define input ranges for uncertainty analysis. The results showed that the Stieber model had the smallest deviation in Vcl. The presence of kaolinite and chlorite in shaly-sand reservoir intervals can result in low gamma-ray readings, while neutron-density (ND) log signatures show fewer uniform readings in the same interval. To provide an accurate description of the formation and geology, a weighted average model called "Stieber-ND" was introduced, with more weight placed on the Stieber model based on borehole conditions. The final Vcl results obtained from the Stieber-ND method showed better alignment with the core data compared to other Vcl models. To verify the results and assess reliability, facies distribution was used, which demonstrated good alignment within the study area. Despite the limited core data available for Vcl calibration, understanding the variations in inputs and their impact on calculations was crucial in developing a robust Vcl model. As more data is acquired, further adjustments can be made to fine-tune the proposed approach, leading to reduced uncertainties in Vcl calculations for the shallow offshore of Suriname.

1 Introduction

The volume of clay (Vcl) is a critical parameter in petrophysical analysis that enables the accurate estimation of other petrophysical parameters like effective porosity, saturation and net-to-gross. This is an important step in characterization of reservoirs as well as valuation of hydrocarbon potentials. Shale is typically defined to be a fine-grained rock composed of silt, clay minerals and other material (organics, heavy minerals etc) [1]. This definition does not describe the mineralogy composition (Kaolinite, illite, smectite) but rather the grain size. Whilst clay can refer to grain size it can also refer to clay minerals, and it is the dual meaning of the word clay that is at the heart of the confusion in the industry. It is therefore important to distinguish between shale volume and clay volume, which are commonly used interchangeably. This distinction (from a petrophysical point of view) is shown in Figure 1 and especially important when dealing with clay-rich sandstone reservoirs. There are three common distribution patterns of clay heterogeneity observed in most reservoirs namely, structural, laminated, and dispersed clays each exhibiting different effects on reservoir properties. All these shale distribution types may occur simultaneously in the same formation. From these three, the dispersed clay largely influences the porosity. Clay minerals also impede porous connections and create heterogeneity both vertically and horizontally. It is thus of crucial importance to establish a robust petrophysical measure able to determine Vcl as accurate as possible.

* Corresponding author: rdjodi@staatsolie.com

Several petrophysical indexes, such as gamma ray, neutron porosity, resistivity, and neutron density as a double clay indicator, can be used to determine clay volume.

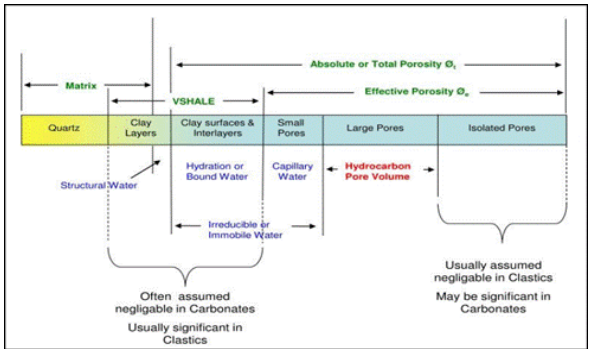

Fig. 1. Porosity definitions [2].

The arithmetic averages from these different indexes are often taken as the clay content close to the actual value. However, it requires caution since the presence of radioactive minerals (other than from clay) in sands will overestimate the clay content calculated from the gamma ray. Clay minerals aren't the only source of gamma ray activity in the formation. As a result, even though natural gamma ray logs are the greatest indicators of clay content, they should be utilized with caution. The presence of gas will lead to underestimations of the clay content calculated from density neutron. If logs are calibrated against mineralogy data analysed on cores (XRD and thin section point data), the inaccuracies in estimating clay content from them can be decreased.

Initially, the volume of clay is calculated using an equation based on a linear relationship, known as the gamma ray index (Equation 1).

$$I_{GR} = \frac{GR_{log} - GR_{min}}{GR_{max} - GR_{min}} \quad (1)$$

Where: IGR is the gamma ray index, GRlog is the gamma ray log reading of formation, GRmin is the minimum gamma ray reading in clean zone, (clean sand or carbonate) and GRmax is the maximum gamma ray reading in shale zone.

Several empirical non-linear calibrated relationships (Fig. 2 & Table 1) have been developed over the years based on geographic and stratigraphic variations. Furthermore, all of these models were developed for specific datasets and have limitations. Therefore, it's important to determine which of these models best fits the available data and input parameters criteria based on the characteristics of the reservoir. Before this study, different approaches were used to determine clay content for different wells in the shallow offshore, resulting in inconsistent outcomes and significant uncertainties in Vcl across the study area. The objective of this research was to establish a more reliable and consistent petrophysical workflow for Vcl calculations. In this project, the volume of clay (Vcl) has been computed using the gamma ray method (Stieber) combined with the neutron – density method. This combination is used to correct for the uncertainties which are raised by using only the gamma ray method or only the neutron – density method, both methods are combined, and a weighted average volume of clay is calculated. This was done based on the Vcl assessment which will be discussed in the methodology section.

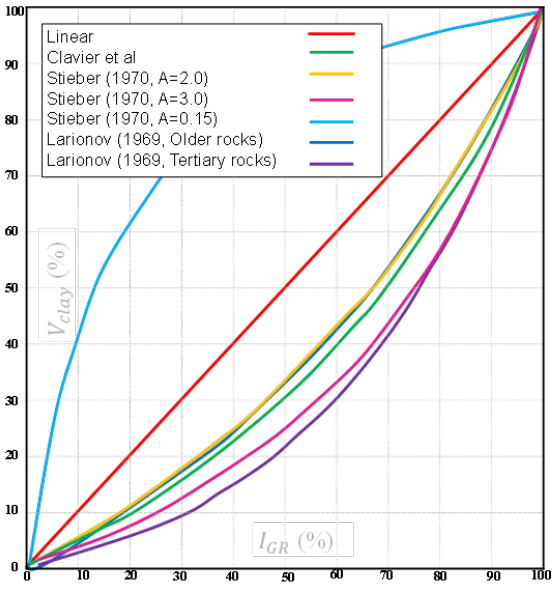

Fig. 2. VCL responses from GR computed by different methods. [3].

2 Geological Background

The study area for this project research is located on the present-day continental shelf of the Suriname-Guyana Basin in water depths from 0 to 60 meters and generally referred to as the Shallow Offshore (SHO) area (Fig. 3). The Shallow offshore acreage has an area size of approximately 41,000 km² span across Suriname's northern coastline, within the north-eastern Atlantic coast of South America, and is bordered by Guyana's territorial boundary to the West and French Guiana's territorial border to the East.

2.1 Geological setting of the study Area

The Suriname–Guyana Basin which encompasses the coastal areas of Suriname and Guyana (Fig. 3), is geographically situated on the northeastern part of the South American continent. The large basin is dominated by its passive-margin setting dating from cretaceous and is comparable to most other Atlantic margin basins. The basin is bordered by the crystalline Guiana Shield, a craton of Proterozoic age, within the southern and is answerable for supplying terrigenous sediment within the basin [4]. The architectural element of the basin is shown in Figure 4. The sedimentary column of the Suriname-Guyana basin forms an eastward monoclinal slope wedge. Towards the NNW, the wedge of sediments increases in thickness up to 8839 m at the basin depocenter located about 150 km offshore.

+

Table 1. Non-linear empirical VCL models.

Model	Comment	Equation	Equation
Clavier	Empirical compromise between the tertiary and older rock equations	$1.7 - \sqrt{3.38 - (I_{GR} + 0.7)^2}$	(2)
Stieber	Built on the foundation that the distribution of clay in sand-stones differs from that in shales, A=2 for older rocks, A=3 for Tertiary rocks and A=0.15 for Cretaceous rocks	$\frac{I_{GR}}{2 - I_{GR}}$	(3)
		$\frac{I_{GR}}{3 - 2 * I_{GR}}$	(4)
		$\frac{I_{GR}}{0.15 - 2 * I_{GR}}$	(5)
Larionov	For older highly consolidated and Mesozoic rocks	$0.33 * (2^{2*I_{GR}} - 1)$	(6)
	For younger unconsolidated tertiary clastic rocks	$0.083 * (2^{3.7*I_{GR}} - 1)$	(7)

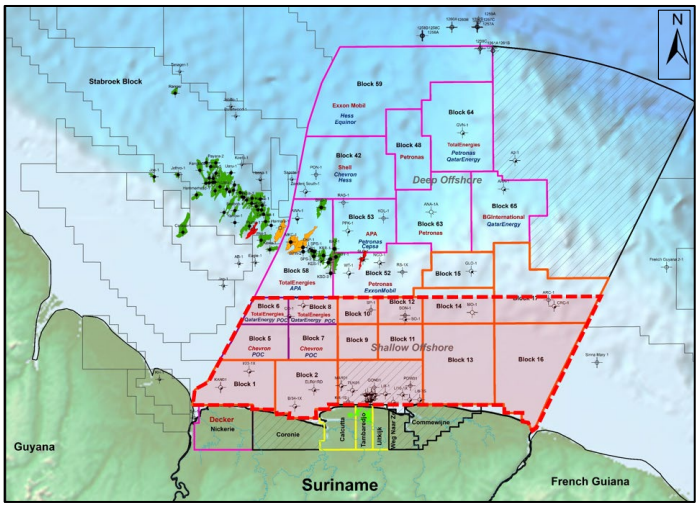

Fig. 3. Study area location map. Indicated by the red dotted rectangular.

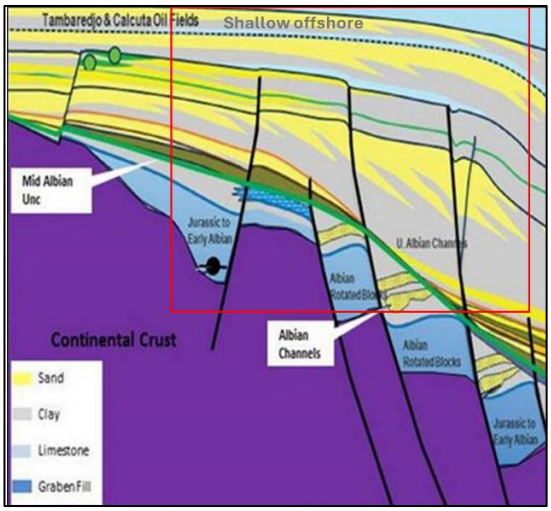

Fig. 4. Architectural elements of the basin. ([4]) The study area is indicated by the red rectangular.

The sedimentary column is often divided into higher order stratigraphic sequences that reflects the 2 major geodynamic evolution phases which is related the Atlantic development: the Central Atlantic and Equatorial Atlantic rifting and spreading [5]. The sediments are primarily clastic, but reef carbonates developed at the paleo shelf edges. The deeper parts of the basin contain turbidite and low-stand fans originating from massive shelf-edge canyons. Remnants of early rifting are present in the form of Jurassic grabens, of which at least two have been identified on the Surinamese shelf: the Nickerie and the Commewijne Grabens. Their onshore equivalent is the Takutu Graben on the border between Guyana and Brazil. These may have been formed as part of a failed-rift system in the early development stages of the basin.

Crawford, 1985 [6] emphasized that there are at least two world-class source rocks of Middle and Upper Cretaceous age, sometimes referred to as the Canje Formation of Cenomanian-Turonian age, found in such sedimentary packages. This source rock is equivalent to the Naparima Hill Formation in Trinidad and Tobago and the La Luna Formation in Venezuela. The Shallow offshore can stratigraphically be divided into five (5) major sequences which are based on tectonic phases and periods of sea level fall in conjunction with biostratigraphy, chrono-stratigraphy, and seismic facies/sequence interpretation:

The five major sequences of the stratigraphy are:

- Sequence 1 - bounded by the Top Jurassic Unconformity at the top; SB-1
- Sequence 2 - bounded by the Mid Cretaceous (Aptian) Unconformity at the top; SB-2
- Sequence 3 - bounded by the Turonian Unconformity at the top; SB-3
- Sequence 4 - bounded by the Maastrichtian Unconformity at the top; SB-4
- Sequence 5 - bounded by the Mid Miocene Unconformity at the top; B-5

This study mainly focused on the sequences four (4) and five (5). Mainly because these sequences have been penetrated by most of the shallow offshore wells and the well results show high prospectivity of these sequences. The area is dominated by a delta plain environment and gradually transitioned to a neritic environment. The nearshore part of shallow offshore exhibits a predominantly delta plain environment, whilst the northern part of the shallow offshore exhibits a predominantly neritic environment, which characterizes a great part of the shelf. The Upper Cretaceous sequence 4

(Coniacian – Maastrichtian) boundary marks a transgressive to a regressive system with increasing sediment input from the southwest. The facies map (Fig. 6) for the Coniacian to Maastrichtian interval exhibits predominantly sandy facies in the south and gradually transitions to a sand-shale alternating facies to the northern of the Shallow offshore. The northern part of this area can be divided into a western part which is predominately shale-sand-silty lithology and an eastern part with more claystone deposition.

The Tertiary sequence (Paleocene - Middle Miocene) which is known as the Sequence 5 interval is characterized by a transgressive environment with high sediment supply towards the western part of the shallow Offshore area which is reflected in the relatively broader delta plain in the west. The facies map (Fig. 5) for the Paleocene to Eocene interval show the sedimentation of alternating sand and shale in the nearshore part of the Shallow offshore with relatively broader sediment influx (Delta Plain) in the west. Moving towards the northern section of the interval, a domination of limestone (mudstone), shale and sand can be observed. The deeper marine environment is dominated by shales, limestones (build ups) and marls. Overall, heterogeneous clastic sequences with varying sand quality and mudstone content can be observed in both sequences.

2.1 Data gathering and validation.

The dataset for this study comprises the following:

- The log-suit of 29 wells, provided by Staatsolie Maatschappij Suriname (Staatsolie). The logging data acquisition for the SHO wells spans five (5) decades and a wide range of data quality is exhibited due to advancements in logging and drilling technology. The data was therefore carefully checked for quality and completeness prior to its use in this study.
- Well reports, petrographic analyses, well header information, core, and cuttings descriptions and high-resolution photos of the cores were all provided by Staatsolie. The mud characteristics, bottom-hole temperature, resistivity of the mud samples, mud filtrate and their corresponding temperatures, mud density, and the bit size are all included in the well header. Along with the above information, formation tops and reservoir data (hydrocarbon density (oil and gas), formation fluid salinity, and drilling mud salinity) were also collected and used.

The data was loaded (Log ASCII (.las) format) into the database of the petrophysical software and thoroughly checked for quality and completeness prior to its use in petrophysical analysis. The quality control process is needed to check if there are problems (depth matching and borehole issues, noises/spikes and cycle skipping) with the data. Prior to log normalization process, it was critical to complete log editing and environmental corrections, with the goal of correcting some recording errors and compensating for environmental effects. After classification of all the available information, unreliable information was discarded. The remaining wells were classified as followed:

- Key wells: wells with complete set of logs (gamma ray, resistivity, and porosity logs) and core data analysis (routine and XRD). These wells are AKT-01, CRC-01 and SP-01.
- Control wells: wells with complete set of logs but without core data analysis.
- Petrophysical well: wells with incomplete set of logs.

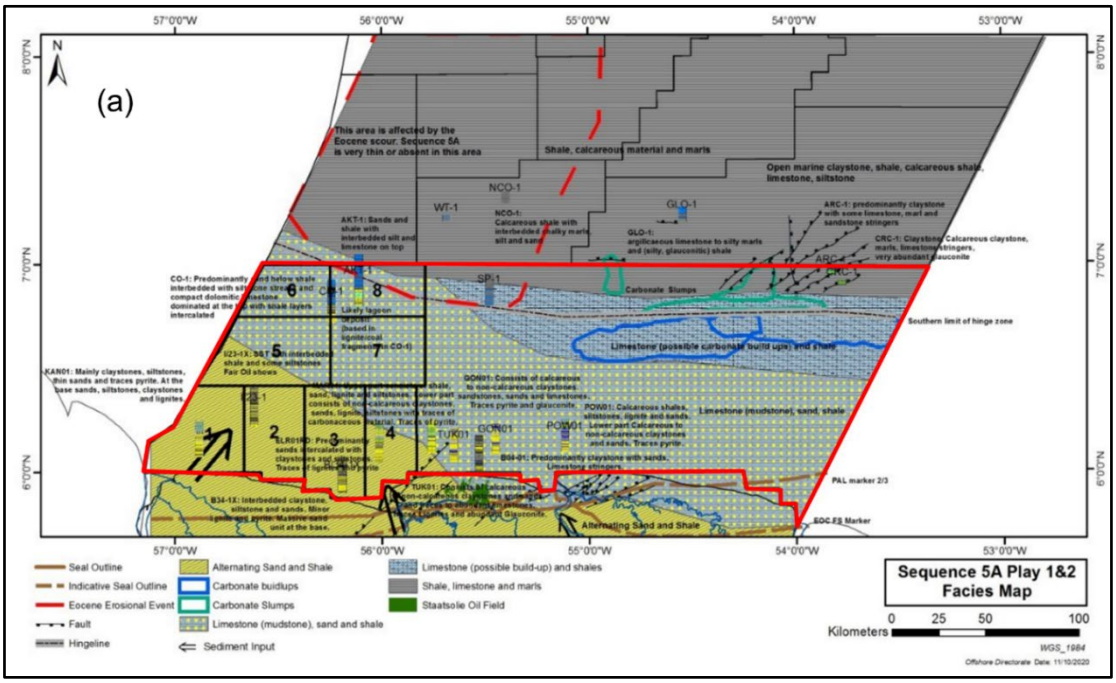

Fig 5. Sequence 5A Play 1&2 (a) facies maps (after [7]).

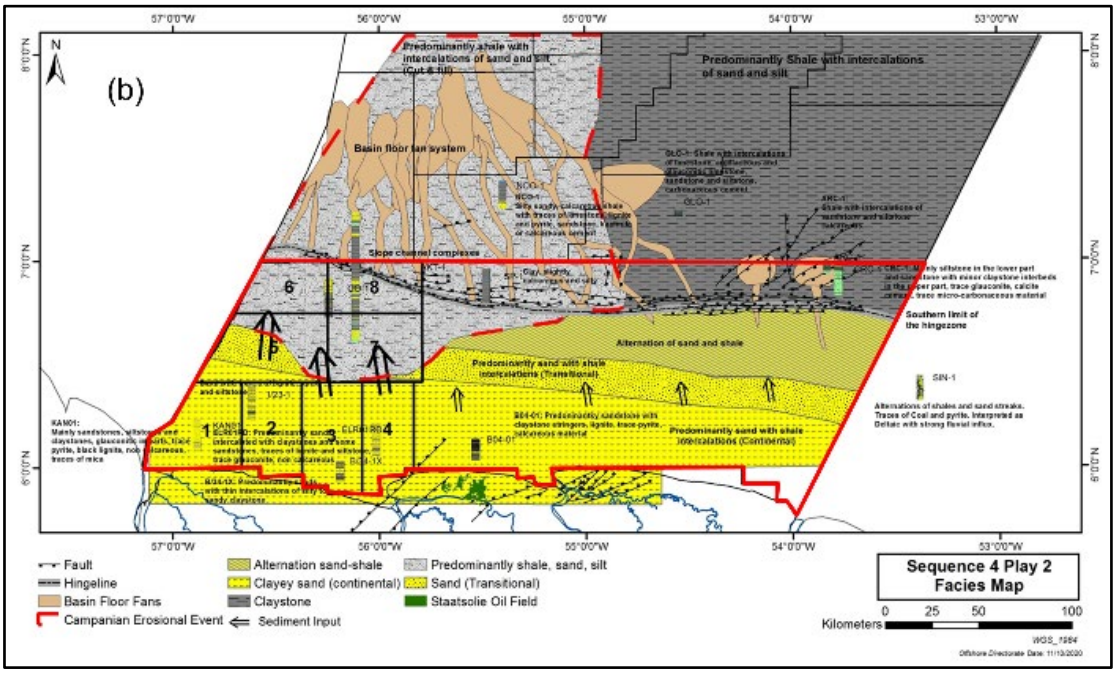

Fig. 6. Sequence 4 Play 2 (b) facies maps (after [7]).

3 Methodology

The calculation of clay volume is usually the first step in log analysis. As mentioned earlier, several empirical non-linear models have been developed based on geographic and stratigraphic—variations to work under specific conditions (certain ages of rocks or certain formations in certain fields). In order to select the most representative model for the shallow offshore area, it was essential to compare the Vcl results calculated from the various models with the Vcl determined from core analysis. This assessment process was carried out for the key wells by using an Excel-based application called "Vclay Equation Assessment Tool (VCLEAT)", built, and created specifically for this project. The VCLEAT spreadsheet is divided into three main tabs namely the input tab, results panel tab and graphical average results tab. The workflow is shown in Figure 7 while the different sections of the tool are illustrated in Figure 8 to Figure 10.

To commence, the assessment necessitated the determination of statistical (mean, P10-P90 percentiles and P5-P95) percentiles for the input parameters. This is done by constructing histograms of the gamma ray, density, neutron, and deep resistivity log curves for each X-ray diffraction (XRD) point, clean sand interval and shaly interval in the geological interval of interest. These statistics were used to define input ranges for the uncertainty analysis. The uncertainty ranges were determined based on the three categories of input data sets in the input data tab (fixed or average values, data ranges and expanded data ranges). The subdivision is important to enhance their impact on each empirical Vcl model.

The statistical mean is required as input for the fixed or average category, the P10-P90 for the data ranges and P5-P95 for expanded data ranges. The calculated Vcl (%) results from the different models/equations per group of inputs (fixed, data ranges and expanded data ranges) are presented in the result tab. A tolerance which indicates the minimum/maximum difference between the core derived Vcl and the calculated Vcl results for each Vcl model per input category can also be seen in the result tab The most optimistic and pessimistic results are highlighted with green and red cell fills, respectively, when compared to each other. The workflow described so far with regard to the input tab and result tab was related to the assessment on one XRD data depth of a relevant well. This process was repeated for all available 64 XRD samples across the three key wells. The graphical average results tab of the VCLEAT tool (Fig. 10) depict the graphical results for all the Vcl results (%) calculated from the various models. The results are compared to an average value of all cores derived Vcl's per well.

The aim is to have all different markers (blue & yellow rectangular, and green dots) as close to the average red line, which provides an indication of the sensitivity of the various input ranges and subsequently an overview of the best fit model(s). The red line represents the average Vcl derived from all the Vcl core values for the specific well while the green markers represent the average Vcl calculated from the various models/equations using the inputs as fixed or average values. The blue rectangular markers represent the average maximum Vcl content calculated from the various models/equations using the data ranges inputs. The yellow rectangular markers represent the average minimum Vcl content calculated from the various models/equations using the expanded data ranges inputs

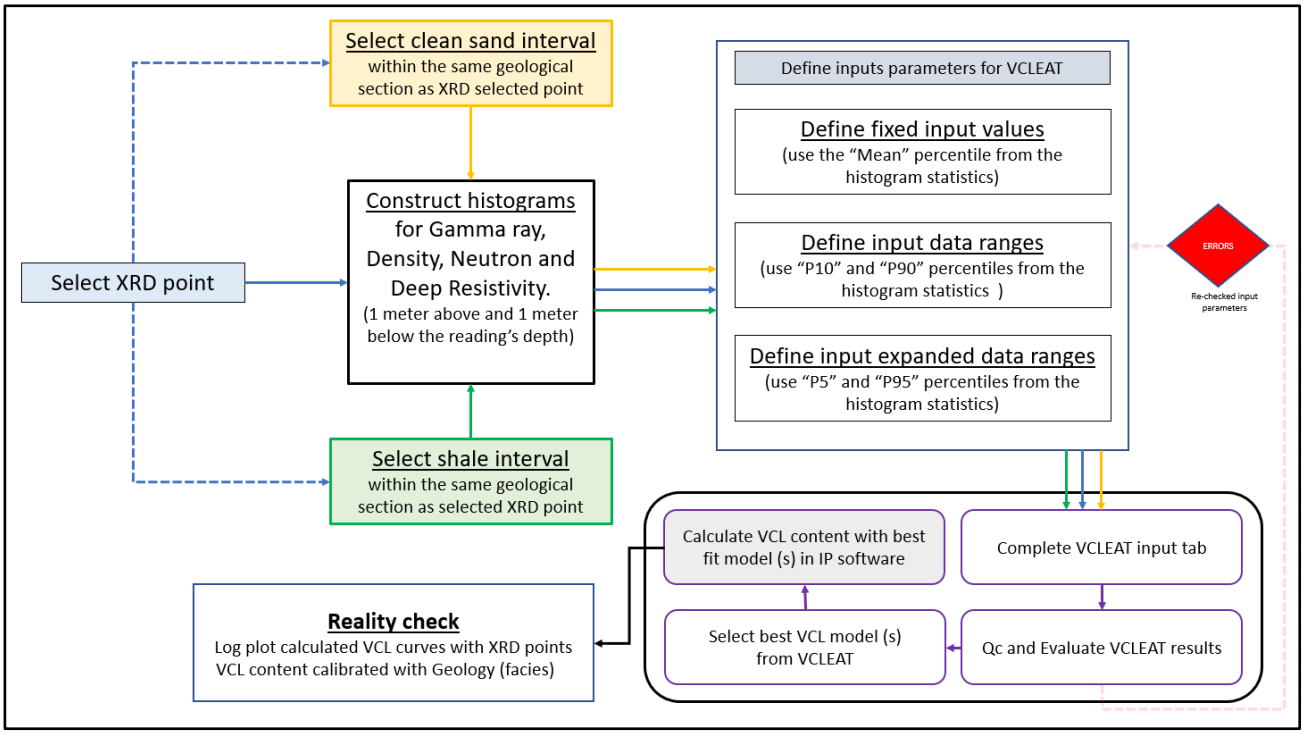

Fig. 7. VCLEAT workflow.

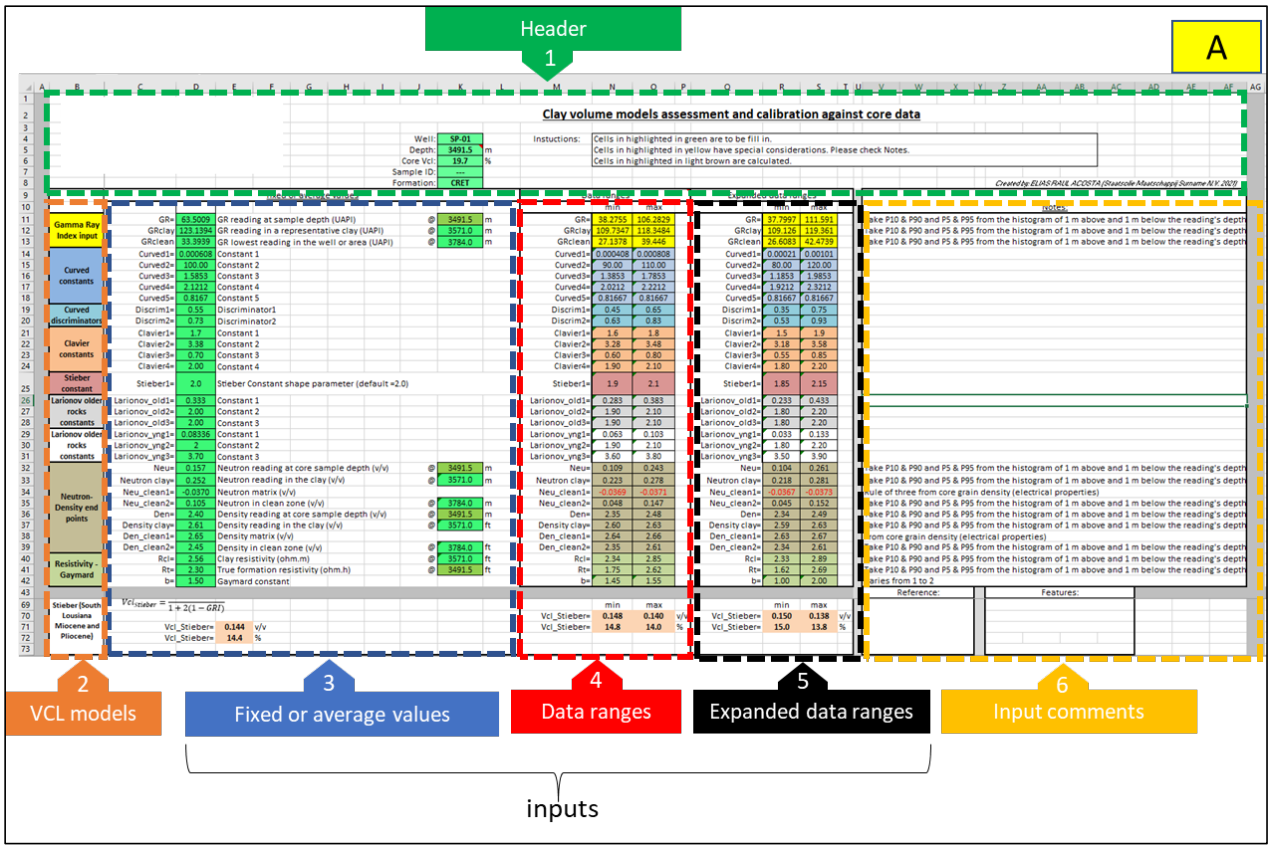

Fig. 8. VCL Equation Assessment Tool (VCLEAT) showing sub-division of the input section (section A).

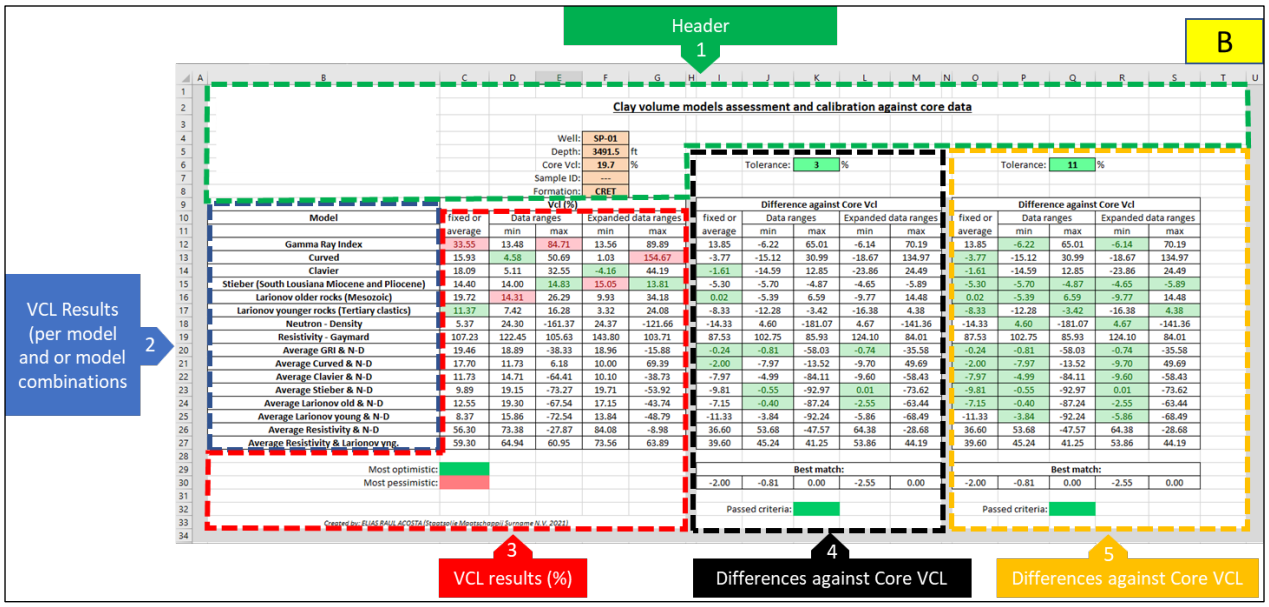

Fig 9. VCL Equation Assessment Tool (VCLEAT) showing sub-division of results panel (section B).

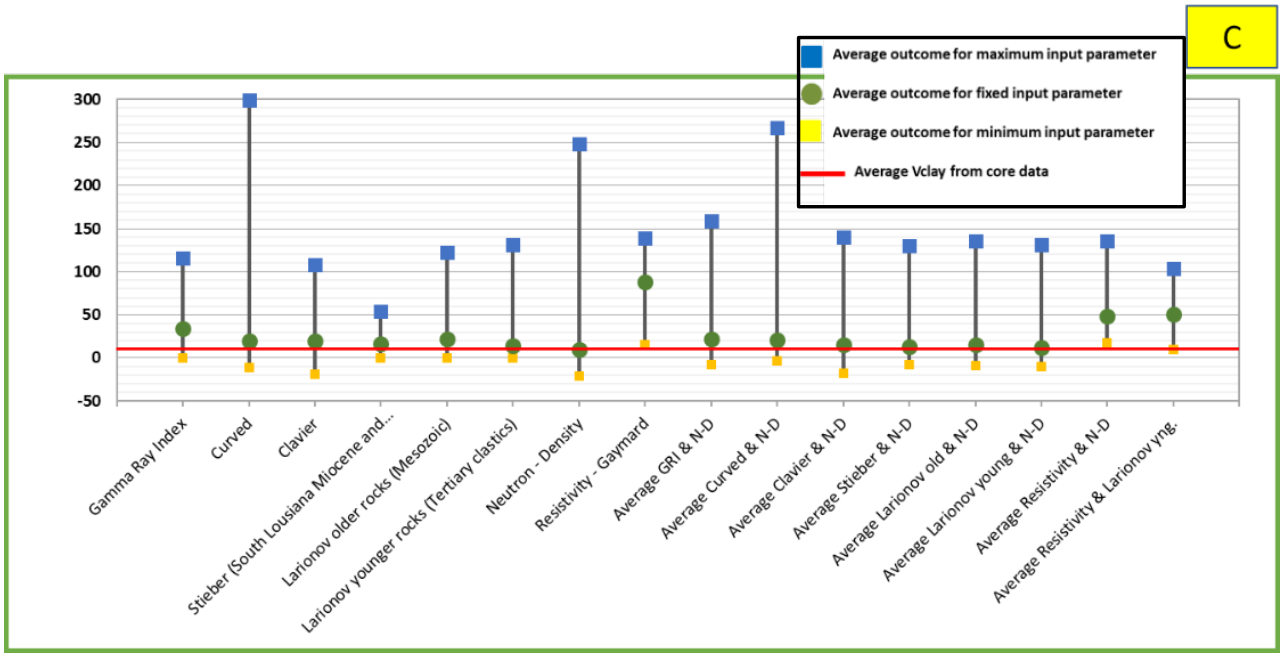

Fig. 10. VCL Equation Assessment Tool (VCLEAT) showing results panel graphically (section C).

4 Results and Discussion

This section deals with a summary of the results and interpretation from the VCLEAT assessment (Figure 11). The figure represents comparisons between Vcl from XRD and the different methods applied in this study to calculate the volume of shale in AKT-01, CRC-01 and SP-01, respectively. As discussed, and explained in the previous section, the best fit models are indicated by the minimum difference between fitted results relative to the mean core line, depicted in red. The mean core line is the average Vcl from XRD per key well. The closer the markers (all together) are to the mean core line, the higher the reliability and sensitivity of the input parameters for the Vcl models. When examining Figure 11, the following observations can be made:

- The Stieber model (highlighted in red) showed the best match with core data confirming that based on the currently available data (which has been used as input parameters), this model best represents the Vcl distribution in the study area for the estimation of Vcl.
- Except for the "Clavier" and "Clavier & N-D" models, it can be observed that all the models would calculate acceptable values for Vcl content by using the minimum input ranges for the parameters. The results from the maximum ranges for the input parameters indicate the opposite. The results demonstrate that the results

are very sensitive to input assumptions and large discrepancies from the core-derived clay content may occur.

- The "Curved" and "average Stieber & N-D" models can respectively be selected as 2nd and 3rd best models for AKT-01. Interestingly, the "Gamma ray Index (GRI)" came as the follow-up best model for CRC-01 well, which quite often yields an over-estimation of clay volume (specially for shallow, young reservoirs), producing an overall pessimistic scenario of the reservoir quality. The "Larionov" younger and older rock models are simultaneously second and third best match models for SP-01. It is important to note that the average "Larionov younger and older rock" and density neutron models are currently the method of choice to determine the Vcl content for the shallow offshore wells. The prior to this study derived Vcl results have been made available and are compared with the results obtained in this study (Figure 12 to 14, track 10, solid magenta curve).

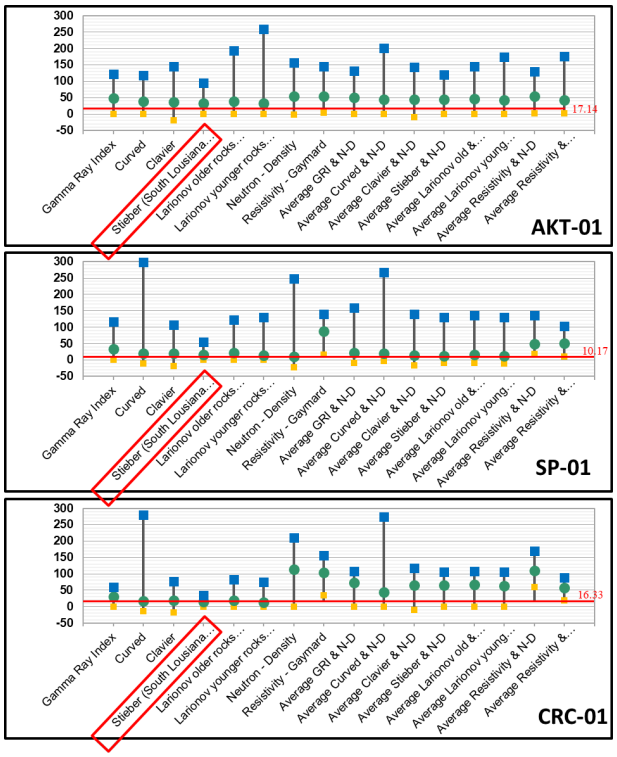

Fig. 11. Graphical summary of VCLEAT results showing the sensitivity of the input parameters on the various Vcl models. Color legend on symbols as per Figure 10.

The next step was to replicate the VCLEAT process in the petrophysical software by using the obtained best match model, in this case Stieber, to estimate the Vcl content of the wells. This approach is a visual interpretation technique with a more qualitative comparison, in which log plots were created to calibrate the obtained results with core data. The resulting Vcl curves are also compared with Vcl values from the gamma ray index (uncorrected) model, and the prior to this study derived Vcl results. Examples of the results of these analyses are shown in Figure 12 to 14, Track 10. The best match fit of the "Vclay Equation Assessment Tool (VCLEAT)" is shown in the log plots presented in Figure 12 to 14 as examples. The Stieber Vcl curve (green curve, track 7) matches well with the core data (red dots in track 7). This conclusion applies to all the 64 samples across the three key-wells. Furthermore, as expected and already pointed out by the "VCLEAT" evaluation, the gamma ray index (olive green curve, track 7) results are systematically higher in all three key wells. However, this difference between the gamma ray index and the Stieber is relatively smaller in CRC-01, as the former was the second-best fit model for this well.

Although the Stieber method turned out to provide the best match by far, it is noticeable that the calculated Vcl curve shows a relatively consistent log (flat or straight) signature across low gamma ray interval (Figure 12, track 1 and 7, 3800m – 3808m). The low gamma ray in combination with the signatures of the resistivity logs (track 4) and porosity logs (track 5 and 6), indicates a dominant sandy interval, that must be relatively homogeneous in nature. However, according to the density-neutron log signatures the sand is probably not as clean as shown by the gamma ray log which is believed to be affected by the presence of clay minerals (kaolinite). The mineralogical composition based on XRD data is depicted in Appendix 1. The presence of kaolinite and chlorite can cause low gamma-ray readings due to the absence of radioactive potassium in these clay minerals. Such presence of clay-minerals does not allow the reservoirs to be considered clean for petrophysical evaluation processes. It is therefore important to have a model in place, which aims to give an accurate and correct description of the formation and geology, but still is general enough to be used on several wells.

The weighted average of the Stieber & N-D Vcl was introduced to cope with the aforementioned issue. This weighted result is obtained by placing more weight on the Stieber curve and consequently less on the density neutron. This weighting approach is completely fair and explainable since the VCLEAT evaluation has demonstrated that the Stieber generally provides good matching with the core data and that the density neutron often needs to be corrected considerably. To explain the weighting procedure, the StieberDN_70-30 curve means that there is 70% weighting on the Stieber approximation and 30% on the density-neutron curve. Figure 12 to 14 (track 9) shows the results of the 50-50, 60-40, 70-30 and 80-20 weighted average calculations plotted against the Stieber and gamma ray index. Yan et al. [8] provide guidelines that make use of borehole conditions to determine the correct amount of weighting that should be applied. Table 2 presents a proposed weighting scheme that can be used based on borehole condition.

A comparison of the weighted average Vcl with the prior to this study derived Vcl content (magenta colour) is shown in Figure 12 to 14 (track 10). Except for SP-01, it can be observed that the Vcl content obtained with the prior to this study Vcl approach (magenta, track 10) is higher and poorly matches the core-data. This may be the result of the Vcl model (Larinov Young/Old Rock) that

was used and choice of the input parameters for the the prior to this study Vcl approach. As for the SP-01 well, the input parameters for the prior to this study Vcl approach may be within the minimum ranges, which brings the Vcl closer to the core average line (Figure 11).

Another potential source of inconsistency during the Vcl calculation process, is a questionable selection of the shale endpoints, which can also cause significant differences in the Vcl calculations.

Table 2. Guidance for borehole condition (modified after [8]) with proposed VCL weightings

Caliper and Bit size (BS) logs	Condition	Proposed VCL weighting for Stieber and Density Neu-tron
Caliper – BS = 0 %	Excellent condition, no need for correction	60 - 40
Caliper – BS < 10 %	Logs are good quality, refer to DRHO log	60 - 40
Caliper – BS =10 – 30%	Logs probably need to be corrected	70 - 30
Caliper –BS >30 – 50%	Logs incorrect, need to correct	80 - 20
Caliper – BS > 50 %	Very bad borehole conditions. incorrect logs	90 - 10

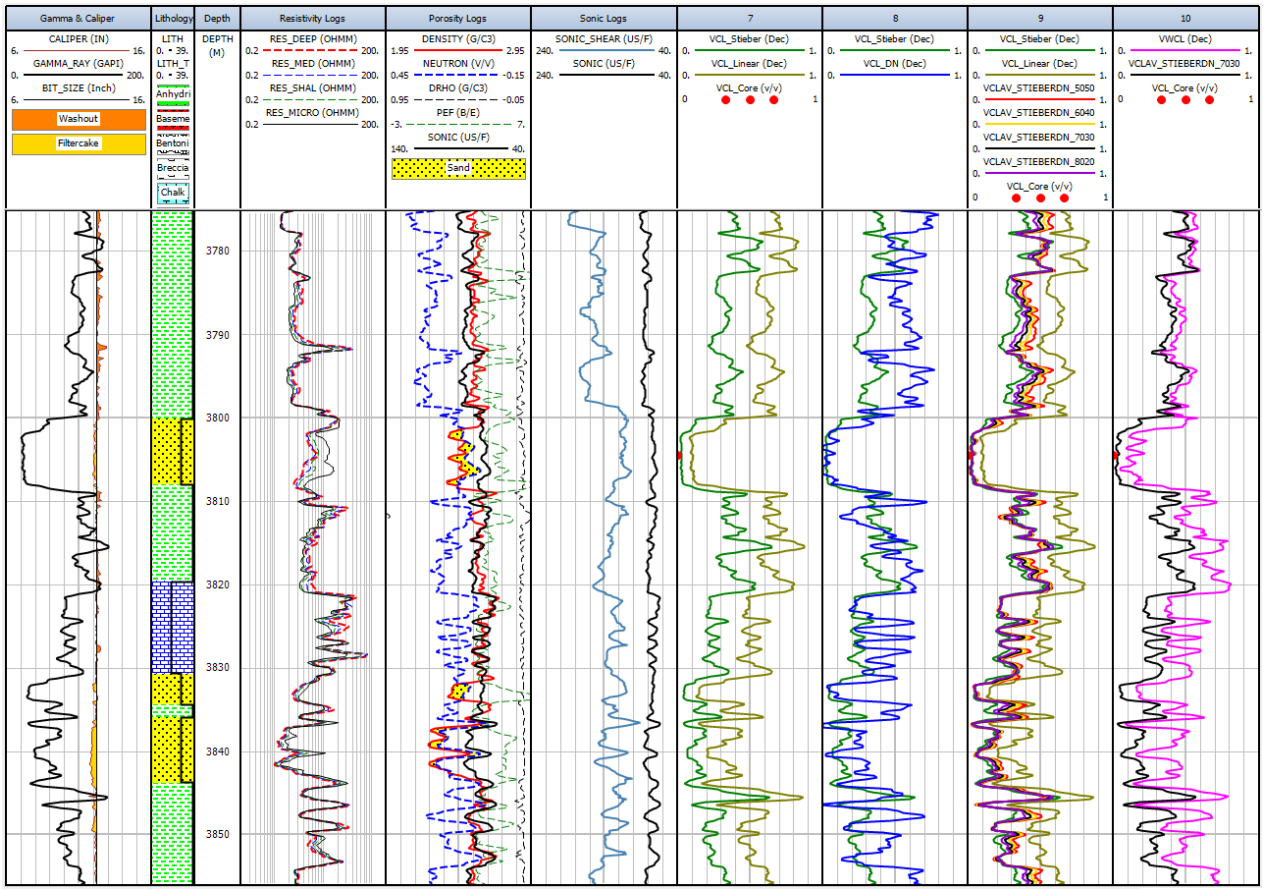

Fig. 12. Log plot example of AKT-01 well showing comparison of obtained VCL contents. From left to right: Track 1: Gamma Ray and Caliper; Track 2: Lithology; Track 3: Depth reference; Track 4: Resistivity curves; Track 5: Sonic, Neutron & Density; Track 6: Sonic logs; Track 7: VCL from Stieber,(solid green line) and VCL from Gamma Ray Index (solid olive-green line); Track 8: VCL from Stieber,(solid green line) and VCL from Density-Neutron (solid blue line); Track 9: VCL from Stieber,(solid green line) and VCL from weighted average (50-50, solid red line; 60-40, solid yellow line; 70-30, solid black line; 80-20, solid purple line); Track 10: VCL weighted average,(70-30, solid black line) and VCL from the prior to this study Vcl approach (solid magenta line); Track 7 to 10: VCL from core (red dots).

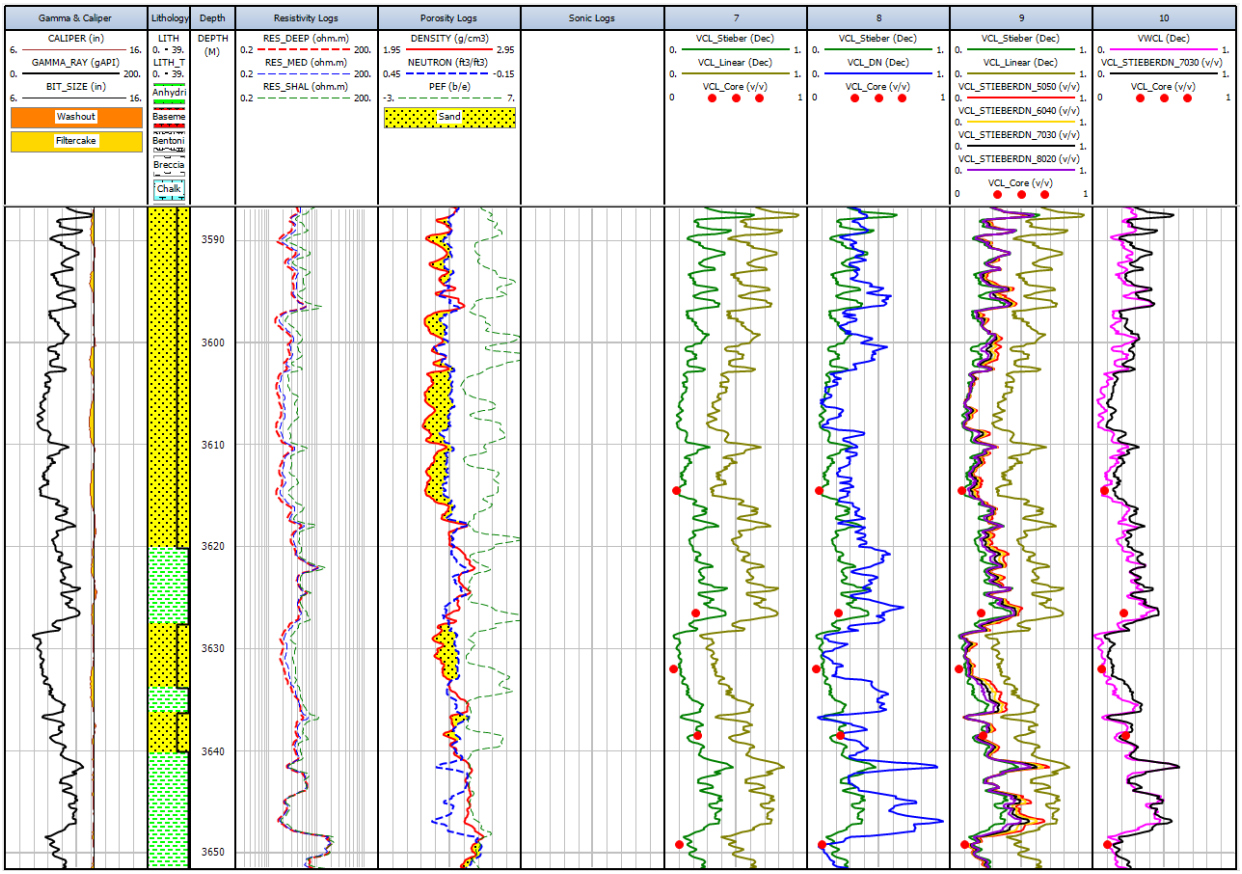

Fig. 13. Log plot example of SP-01 well showing comparison of obtained VCL contents. From left to right: As per Figure 12.

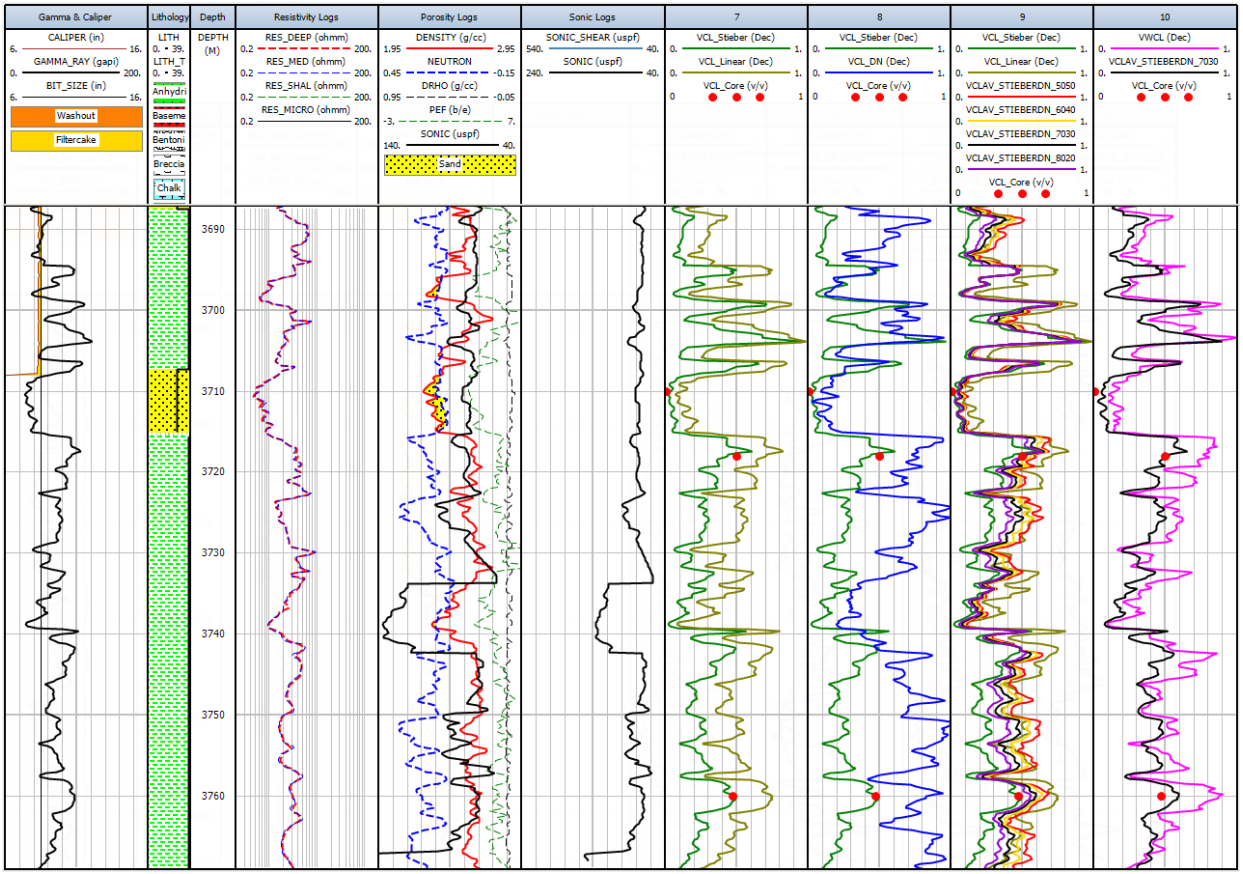

Fig. 14. Log plot example of CRC-01 well showing comparison of obtained VCL contents. From left to right: As per Figure 1.

To ensure that the weighted average Vcl method gives consistent results, it proved necessary to also apply it to the other geological zones without core Vcl data in the control and petrophysical wells. The wells are then ranked from lowest Vcl content to highest Vcl content based on geological interval (Figure 15). Finally, it was verified that the results matched the facies distribution maps in the studied intervals, the Paleocene-Eocene and Cretaceous strata (Figure 16 and Figure 17).

Figure 15 shows that the CRC-01, SP-01, GLO-01, AKT-01 and WT-01 wells, all in the deeper waters of the shallow offshore area, have the highest Vcl content. As illustrated by Figure 16 and Figure 17, these wells occur in clay-rich facies regions. The Paleocene Eocene interval in well AKT-01 is a limestone dominant section with very low Vcl content. In conclusion, the log derived Vcl estimates calculated with the weighted average method clearly reflects the lateral clay distribution in the study area and, of all the empirical methods tested, provides the best match with the facies distribution maps for the various geological intervals.

5 Conclusion

This study developed the VCLEAT workflow to evaluate Vcl sensitivity. This workflow facilitated the investigation of how variations in Vcl calculation inputs impact the results. The workflow identified the Stieber model as exhibiting minimal deviation (64 XRD samples) from core data measurements and demonstrated the most stability when incorporating variations (smaller range between minimum and maximum values). However, a challenge arose in intervals with low gamma-ray signatures due to the presence of kaolinite/chlorite. To address this, a weighted average Vcl approach (Stieber-ND) was introduced, assigning greater weight to the Stieber model based on borehole conditions. This method demonstrably improves Vcl estimates, achieving the best overall agreement with both core data and facies distribution.

The authors would like to thank Staatsolie Maatschappij Suriname N.V for the permission to use data for this project. The authors would also like to acknowledge special thanks to Mr. Jan E. Lutgert for his untiring input and guidance through the execution of this project, the Anton de Kom university of Suriname, and the reviewers who kindly reviewed the manuscript and provided valuable suggestions and comments.

References

1. E. Donaldson and D. Tiab, *Basic Well-Log Interpretation*, (2012)
2. Senergy, *Deterministic Petrophysics PowerPoint presentation*, (2015)
3. Martins, J. L., Castro, T. M., Emperical and petrophysical models for shaliness estimation in clastic sedimentary rocks, *Sociedade Brasileira de Geofisica,* (2018)
4. Staatsolie, www.staatsolie.com, (2024). [Accessed 24 August 2022]
5. Staatsolie Exploration Division, Staatsolie, *SHO Central and East PI Update Report November 2021*, (Unpublished).
6. C. R. Scotese and G. Jan, *Paleogeographic Atlas,* (1992)
7. F. D. Crawford, C. E. Szelewski and G. D. Alvey, *Geology and exploration in the Takutu Graben of Guyana Brazil,* (1985)
8. E. Anderson, J. Yan, R. Lubbe, K. Water and N. Pillar., Log quality assessment and data correction for AVO, *10 th EAGE Conference and Exhibition, Rome Italy.,* (2008).

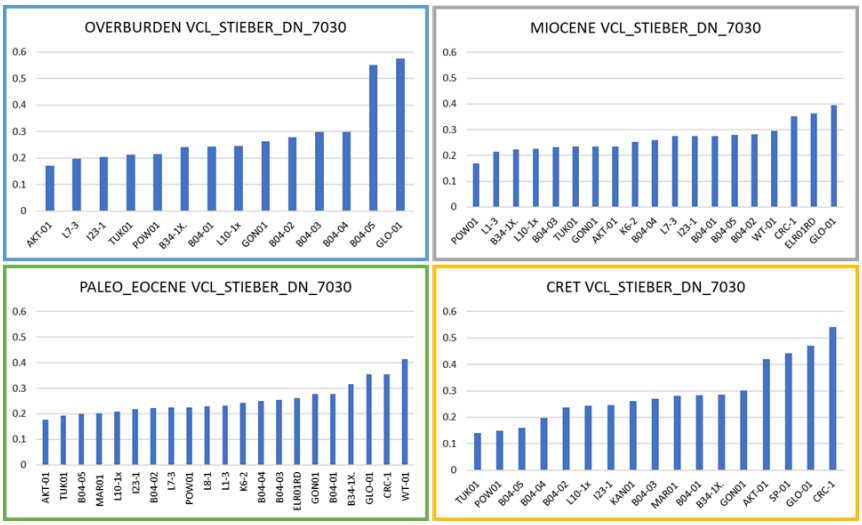

Fig. 15. Ranking of calculated VCL content using the weighted average Stieber-Density-Neutron method.

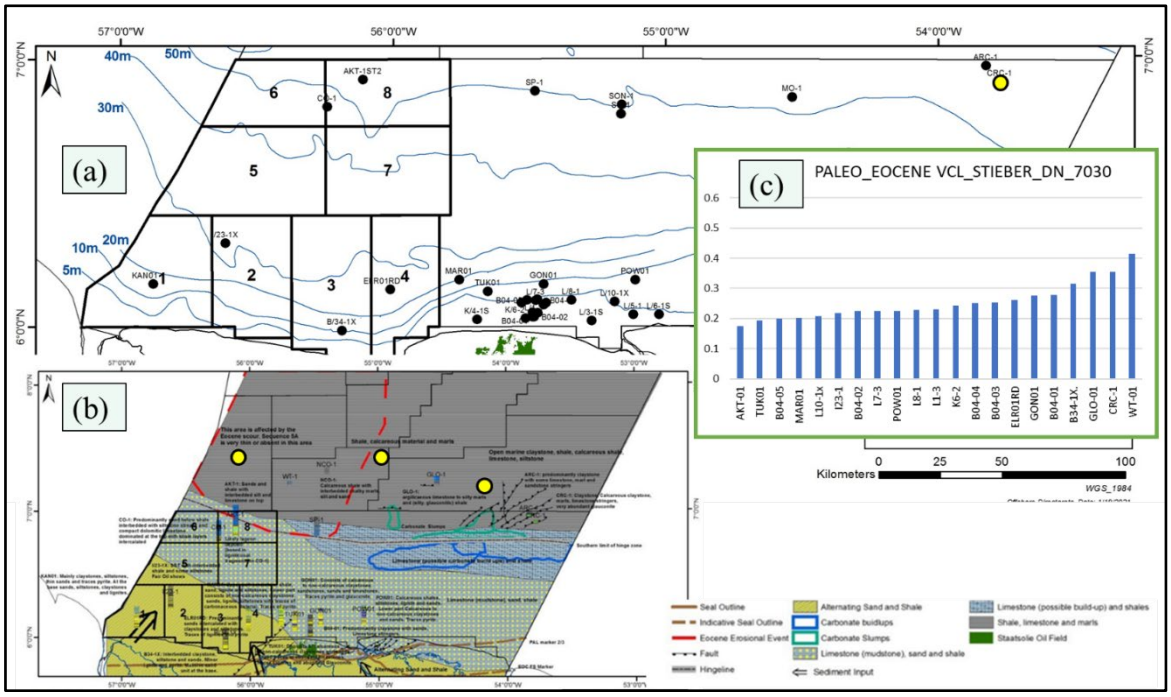

Fig. 16. VCL distribution on the well location map (a) and facies map (b) after VCL ranking for all well across the Paleocene-Eocene interval.

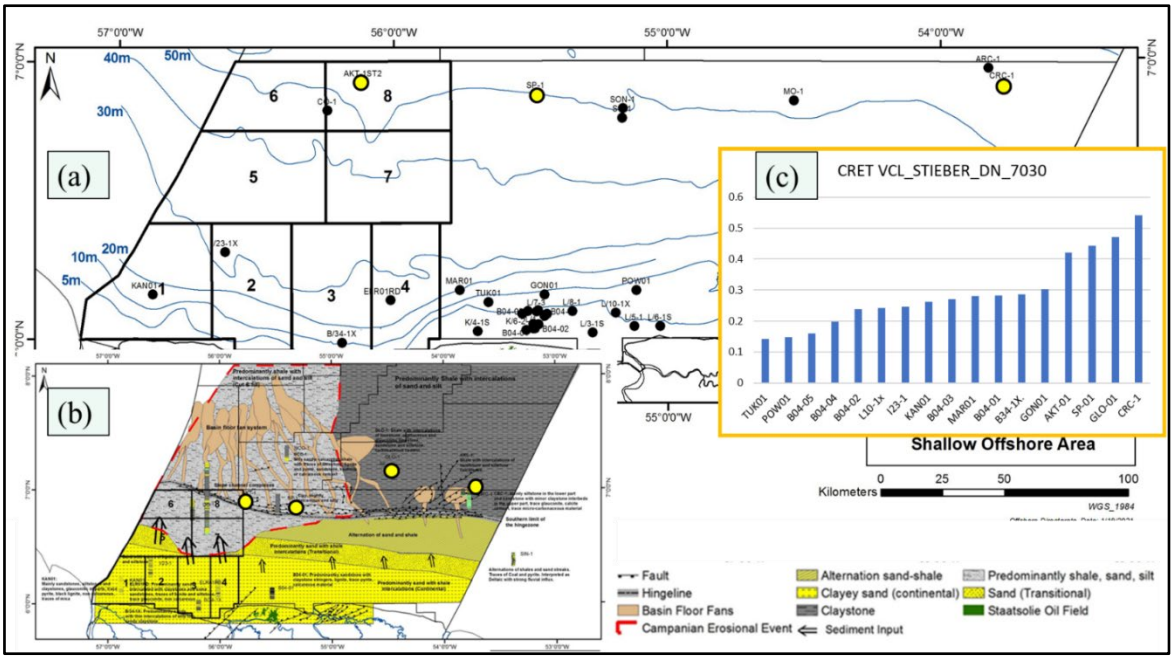

Fig. 17. VCL distribution on the well location map (a) and facies map (b) after VCL ranking for all well across the Cretaceous interval.

Appendix 1: Mineral composition (vol percentage) as per XRD and thin section analysis for the three key wells.

Wells	Chlorite	Kaolinite	Illite	Mx US*	Smectite	*Subtotal*	Calcite	Dolomite	Siderite	Ankerite	*Subtotal*	Quartz	K-spar	Plagioclase	Muscovite	Biotite	Heavy Minerals*	*Subtotal*
CRC-01	1.4	8.6	3.1	2.6	3.2	*19.0*	1.3	5.3	0.5	0.0	*7.1*	44.9	9.6	19.4	0.0	0.0	0.0	*73.9*
AKT-01	0.7	4.4	2.5	3.2	0.0	*10.8*	1.8	6.9	0.5	1.2	*10.5*	63.9	4.6	9.3	0.5	0.2	0.1	*78.6*
SP-01	4.3	2.1	2.2	0.1	0.0	*8.7*	10.2	0.5	0.5	4.5	*15.7*	55.2	4.5	14.9	0.6	0.2	0.2	*75.6*